Effect of the transient mobility in one-dimensional continuum deposition

1998 J. Phys. A: Math. Gen. 31 1165

(http://iopscience.iop.org/0305-4470/31/4/007)

J. Phys. A: Math. Gen. **31** (1998) 1165–1179. Printed in the UK PII: S0305-4470(98)85721-1

Effect of the transient mobility in one-dimensional continuum deposition

Daniel H Linares, Raul H Lopez and Victor D Pereyra†

Departamento de Física and Centro Latinoamericano de Estudios Ilya Prigogine, Universidad Nacional de San Luis, Chacabuco 917, CC:136, 5700 San Luis, Argentina

Received 7 July 1997, in final form 8 October 1997

Abstract. We study the kinetics and the jamming state in the continuum deposition of molecules which present transient mobility, i.e. *hot* molecules. The transient mobility is caused by the inability to dissipate the energy gained by the particle after formation of the surface bond instantaneously. Accordingly, the particle flies up to a distance R before being immobile. We analyse the continuum deposition of *hot* monomers in one dimension. The rate equations for the gap distribution functions are written and solved by means of numerical procedures and the results are compared with Monte Carlo simulations. The kinetics of the process show a crossover between power-law and exponential asymptotic regimes for increasing values of R. The jamming state presents a jamming density $\rho_R(\infty)$, which is strongly dependent on the parameter R.

1. Introduction

Models of irreversible monolayer deposition (or adsorption) of particles on solid surfaces have been investigated extensively [1–9]. In many experiments on the adhesion of colloidal particles and proteins on solid substrates the relaxation time scales are much longer than the times for the formation of the deposit. Well known examples of irreversible monolayer deposition models are 'random sequential adsorption' (RSA) [1] and the 'car parking problem' [1, 9]. In these models, rigid particles are placed at random, sequentially and irreversibly onto solid smooth surfaces in such a way that the particles do not overlap. If an incoming particle approaches part of the substrate which is already covered, it is rejected. Eventually no more particles fit on the surface and the process stops in the so-called *jamming* (or saturation) limit. The quantity of interest is the fraction of total area, $\theta(t)$, covered in time t by the depositing particles or objects. Due to the blocking of the area by the already randomly adsorbed particles, the limiting or 'jamming coverage', $\theta_j(\infty)$, is less than that corresponding to close packing. The emergence of this jammed state is influenced by infinite memory effects. Consequently, its formation cannot be described by mean-field theory, except for very early times, when $\theta \propto t$. The analysis of such models includes theoretical studies and computer simulations. Experimental results, as for example the adhesion of latex spheres on a silica surface [10], support the models as possible theoretical tools to treat the irreversible adsorption. The analytical treatment includes exact solutions [3, 9], which are mostly in one dimension, series expansion, shielding and truncation [1], etc, while Monte Carlo simulations have been used extensively in the analysis of the RSA problem [1].

† To whom all correspondence should be addressed.

0305-4470/98/041165+15$19.50

On the other hand, the analysis of the transient mobility on the irreversible deposition is interesting. One possible mechanism which involves transient mobility is diffusional relaxation. The molecules, after adsorption on surface sites, jump by thermal activation to a more favourable energy location, i.e. stronger adsorption sites, where they remain irreversibly adsorbed. The effect of diffusional relaxation on RSA processes has been introduced and discussed by Privman and Nielaba [11] in the RSA of dimers in a one-dimensional (1D) lattice, where as a main feature, full coverage is reached. The analysis is also extended to 1D k-mer deposition [12], adsorption of particles on a two-dimensional (2D) square lattice [13] and dimer deposition on different fractal structures [14]. More recently, the effect of diffusional relaxation was introduced by Mann *et al* [15] in the irreversible deposition of small latex particles, to explain the inconsistency between the behaviour of the radial distribution function and the variance of the density of adsorbed particles.

Another well studied relaxation mechanism is so-called 'hot adsorption'. Experimentally, scanning tunnelling microscopy (STM) observations [16] of the adsorption of O_2 on Al(111) have shown that, under certain conditions, oxygen molecules striking the metal surface not only dissociate instantaneously upon adsorption, but dissipate part of their excess energy in degrees of freedom parallel to the surface. As a consequence, the resulting monomers fly apart up to a distance R before being immobily adsorbed. The experiment has shown that at a temperature $T = 300$ K, the travelling distance R is, on average, approximately 40 Å for each monomer. 'Hot' adsorption has also been observed by Weiss and Eigler [17]. They have reported that Xe atoms travel several hundreds of angstroms across the Pd(111) surface, kept at 4 K, before adsorption. We can conclude that the inability to dissipate the energy gained by a particle after formation of the surface bond instantaneously results in transient mobility relaxation.

This interesting process has been described in the framework of the random sequential adsorption model. Monte Carlo simulations have been performed to analyse 1D and 2D hot dimer adsorption [18, 19]; the results show that both the kinetics and the saturation state are strongly dependent on R. On the other hand, an analytical treatment of this process has only been performed in one dimension [20, 21]. Numerical simulation has shown that the hot dimer mechanism considerably enhances the rate of CO_2 production in the catalysed oxidation of carbon monoxide [22]. The influence of such an adsorption mechanism has also been used to analyse the critical behaviour in the monomer–dimer irreversible phase transition [23]. The authors have found that the critical threshold of the second-order irreversible phase transition (IPT) and also the location of the first order IPT depend on R. However, the evaluated critical exponents indicate that the universality class of the transition remains unchanged.

The analysis of 'hot' relaxation is also extended to continuum deposition. Recently, 'hot' dimer adsorption in the continuum has been analysed by means of numerical simulations and analytical approaches for finite flight distance R [24]. The jamming state, as in the discrete state, depends on the parameter R; however, one of the most interesting features which differentiates the continuum deposition from RSA of the hot dimer in the lattice is the piecewise profile which characterizes the jamming density as a function of the flight distance R. The structure observed in the profile presents finite discontinuities in the neighbourhood of the integer values of R, which is explained by the fact that the probability to cover the gaps of length $2R$ is extrictly zero, and the number of gaps of size nR (with n integer) are relatively high.

Based on the results observed in the hot dimer continuum deposition, we are interested in extending the study of the 'hot' relaxation mechanism to the continuum deposition of molecules (monomers) in one dimension.

The paper is organized as follows. First, we describe in section 2 the model of monomer adsorption in one dimension, in particular we develop and solve the kinetics rate equations for $R < \sigma$; the generalization of the treatment to any values of R is given in the appendix. The simulation scheme is also presented in this section. The results for both the kinetics and the jamming state are given and discussed in section 3. Finally, in section 4 we present our conclusions.

2. The model

Let our model consider the deposition of hot monomers in a one-dimensional infinite lattice. The area covered by the monomer is taken to be equal to σ. The monomers arrive randomly at the line at a rate w (per unit time per unit length). If an incoming monomer is blocked by an adsorbed adparticle, it is removed; otherwise the deposition is successful. After deposition in a free area, the monomers fly apart up to a certain distance R (in terms of σ units) as in the discrete version of the hot deposition process. If during the flight one monomer hits another adparticle or a cluster of adparticles which are already at rest on the surface, the flying monomer is frozen in the collision point (see figure 1). Note that the concept of jumps has also been introduced in previous RSA studies. In fact, Pagonabarraga *et al* [25] have considered a model where particles arrive at the line forming an angle α with the normal; the authors argue that the fixed values for α are induced by the presence of a driving external field. However, the similarity between both models is restricted to the fact that, in both cases, particles move instantaneously from the original landing point to the definitive deposition or adsorption place.

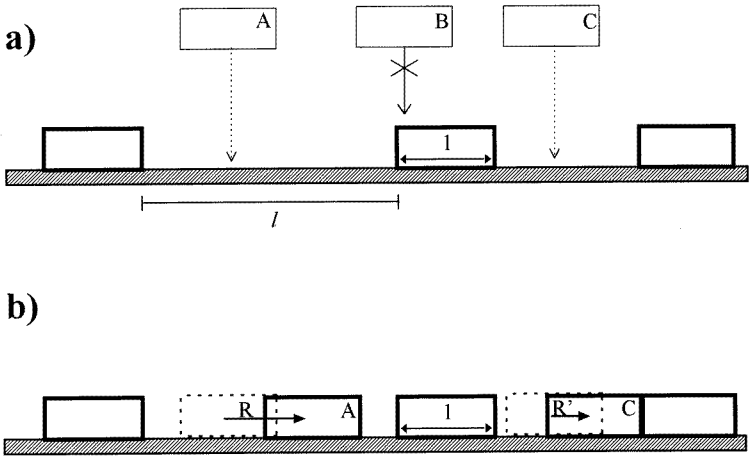

Figure 1. Illustration of the deposition process. (a) The incoming monomer A of size 1 arrives at the line and its centre is deposited in $(l - 1)$ possible places. The monomer B is blocked by a previous adsorbed particle, therefore the adsorption process is aborted. (b) After deposition, the monomer flies apart up to a distance R from the deposition place (monomer A) before being made immobile. If during the flight the particle hits another adparticle or cluster of adparticles which are already at rest on the line, the flying monomer is frozen in the collision point (monomer C) and the flying distance is $R' < R$.

The kinetics of the hot monomer adsorption process are monitored following the time evolution of $\bar{G}_R(\bar{l},\bar{t})\,\mathrm{d}\bar{l}$, which represents the number density of gaps with length between $\bar{l}$ and $\bar{l}+\mathrm{d}\bar{l}$ at time $\bar{t}$, for a given value of R. The number density of gaps per unit length is given by

$$n_R(t)=\int_0^\infty G_R(l,t)\,\mathrm{d}l \tag{1}$$

where, for convenience, we have introduced the dimensionless variables $t=\sigma w\bar{t}$, $l=\bar{l}/\sigma$ and $G_R=\sigma\bar{G}_R$. In the following, we consider $\sigma=1$ without loosing generality.

The density $\rho_R(t)$ is also related to the fraction of uncovered surface, i.e. the fraction of the line uncovered by the adsorbed particles,

$$\rho_R(t)=1-\int_0^\infty lG_R(l,t)\,\mathrm{d}l. \tag{2}$$

Due to the nature of the deposition process, that is, one monomer can hit another adparticle or cluster of adparticles leading to cluster formation, each gap does not correspond necessarily to one particle, so we then have $\rho_R(t)\neq n_R(t)$.

According to the definition of the model, the kinetics of the process are given by the time evolution of $G_R(l,t)$. To illustrate the method, we present in the following subsection the derivation of the rate equations and their solution for the case $R<1$. In the appendix, we present the derivation of the case $R>1$.

2.1. Rate equations for $R<1$

The rate equations for the gap distribution function (GDF) can be written in a closed form by considering all the ways in which intervals may be created or destroyed during the process. Let us now write the set of equations that describe the kinetics evolution of the GDF for $R<1$:

for $R<1<l$

$$\frac{\partial G_R^0(l,t)}{\partial t}=-(l-1)G_R^0(l,t)+RG_R^0(l+1,t)+\int_{l+1}^{l+R+1}G_R^0(l',t)\,\mathrm{d}l'+2\int_{l+R+1}^{\infty}G_R^0(l',t)\,\mathrm{d}l' \tag{3}$$

for $R<l<1$,

$$\frac{\partial G_R^1(l,t)}{\partial t}=RG_R^0(l+1,t)+\int_{l+1}^{l+R+1}G_R^0(l',t)\,\mathrm{d}l'+2\int_{l+R+1}^{\infty}G_R^0(l',t)\,\mathrm{d}l' \tag{4}$$

and finally, for $0<l<R$,

$$\frac{\partial G_R^2(l,t)}{\partial t}=lG_R^0(l+1,t)+\int_{l+R+1}^{\infty}G_R^0(l',t)\,\mathrm{d}l'. \tag{5}$$

In equation (5) the gaps can be created from those with length $l'=l+1$ by deposition of one monomer in the l possible inner places. Creation of such gaps also takes place by deposition of the centre of a monomer at distance $l+R+1/2$ from one extreme of a given gap; in this case the minimum possible length for such gaps will be $l'=l+R+1$, and the integration takes into account the contribution of those gaps with length $l'\geqslant l+R+1$. Note that gaps with length between $0<l<R$ cannot be destroyed because $R<1$.

The analysis of the first terms in equation (4) is similar to the first terms of equation (5) but the possible deposition locations for a given monomer are R instead of l. The second

term in equation (4) represents the increment in the number of gaps with length between $R < l < 1$ by destruction of gaps with lengths $l+1 < l' < l+R+1$. As is described above, the event takes place by deposition of a given monomer whose centre falls at a distance of $l - R + 1/2$ from one of the extremes of the gap. The next term is due to the contribution of the gaps with length $l' \geqslant l + R + 1$; the factor of two is due to the fact that the centre of a given monomer can be deposited in two possible places located at $l \pm R + 1/2$.

Finally, in equation (3) we describe the time evolution of the distribution function of gap with length $l > 1 > R$. The first term of equation (3) takes into account the destruction of the gap by deposition of a given monomer in $(l - 1)$ possible inner places. The second, third and fourth terms in equation (3) are equivalent to those of (4).

To solve the set of integrodifferential equations, we have used a standard procedure [1–3]. Let us consider equation (3), which describes the evolution of gaps with length $l > 1$. Inserting the following ansatz,

$$G_R^0(l,t) = H(t)t^2\,\mathrm{e}^{-(l-1)t} \tag{6}$$

in equation (3) gives

$$\frac{\mathrm{d}H(t)}{\mathrm{d}t} = H(t)\left[R\,\mathrm{e}^{-t} + \frac{1}{t}(\mathrm{e}^{-t}(\mathrm{e}^{-Rt}+1) - 2)\right] \tag{7}$$

the solution of which is

$$H(t) = \mathrm{e}^{R(1-\mathrm{e}^{-t})}\exp\left[\int_0^t (\mathrm{e}^{-(R+1)u} + \mathrm{e}^{-u} - 2)\frac{\mathrm{d}u}{u}\right]. \tag{8}$$

Introducing the exponential-integral function

$$E_1(t) = \int_t^\infty \mathrm{e}^{-u}\frac{\mathrm{d}u}{u}$$

the function $H(t)$ can be rewritten as

$$H(t) = \frac{\mathrm{e}^{-(2\gamma-R)}}{(R+1)t^2}\mathrm{e}^{-[E_1((R+1)t)+E_1(t)+R\,\mathrm{e}^{-t}]} \tag{9}$$

where $\gamma = 0.577\,24\ldots$ is the Euler constant. Once $G_R^0(l,t)$ is known, equations (4) and (5) can be easily solved to obtain the following expression for $G_R^1(l,t)$ and $G_R^2(l,t)$:

$$G_R^1(l,t) = \int_0^t H(t')t'\,\mathrm{e}^{-lt'}(Rt' + \mathrm{e}^{-Rt'} + 1)\,\mathrm{d}t' \tag{10}$$

and

$$G_R^2(l,t) = \int_0^t H(t')t'\,\mathrm{e}^{-lt'}(t'l + \mathrm{e}^{-Rt'})\,\mathrm{d}t'. \tag{11}$$

In figure 2 we have shown the behaviour of the gap distribution functions $G_R^0(l,t)$, $G_R^1(l,t)$ and $G_R^2(l,t)$ as a function of l, for fixed value of R and with time t as a parameter. The mean feature of the l dependence of the GDF is the finite discontinuity which appears in $l = R$ at any time t, which is due to the creation of gaps with length $l < R$ taking place by deposition of a given monomer, the centre of which falls at a distance of $l+1/2+R$ from one of the extremes of the interval, while for the gaps with length $R < l < 1$ the possible deposition places are located at a distance $l + 1/2 \pm R$; therefore, in the neighbourhood of $l = R$ the number of gaps with length $l > R$ is bigger than those with length $l < R$. At the end of the process ($t = \infty$), another discontinuity appears at $l = 1$ because there are no intervals larger than 1 ($G_R^0(l,\infty) = 0$ for $l > 1$). One important consequence of the 'hot' adsorption mechanism is that the gap distribution function $G_R^2(l,\infty)$ does not present

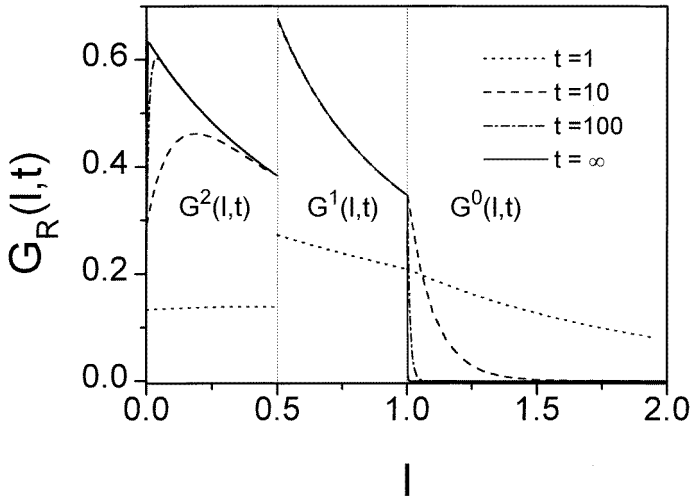

Figure 2. The gap distribution function (GDF) $G_R(l,t)$ as a function of l, with time t as a parameter and for fixed values of the flying distance $R = 0.5$. We can observe the finite discontinuity at $l = R$ for any value of time, and at $l = 1$ for $t = \infty$.

logarithmic divergence at contact due to the fact that the particles can hit each other. At the limit $R = 0$ corresponding to classical RSA, $G_R^2(l,\infty) = 0$ by definition (see equation (11)) and $G_0^1(l,\infty) \propto -\ln(l)$ for $l \to 0$ as we expect [26–28].

Is interesting to note that the last arguments are also valid for $R > 1$; however, in these cases the first discontinuity will be located at $l = R - \mathrm{int}(R)$ (where the function $\mathrm{int}(R)$ means the integer part of R), that is, because gaps with length $l < R$ are filled by particles which hit one of the extremes of the interval, at $t = \infty$ the length of the resulting gap will be $l = R - \mathrm{int}(R)$.

From the gap distribution function, it is possible to obtain the density $\rho_R(t)$ by using equation (2) as

$$\rho_R(t) = 1 - \int_0^R lG_R^2(l,t)\,\mathrm{d}l - \int_R^1 lG_R^1(l,t)\,\mathrm{d}l - \int_1^\infty lG_R^0(l,t)\,\mathrm{d}l. \tag{12}$$

An alternative route which allows the analysis of the short-time and asymptotic behaviour of the process is by using the kinetic equation satisfied by the density $\rho_R(t)$, which can be written as

$$\frac{\mathrm{d}\rho_R(t)}{\mathrm{d}t} = \Phi_R(t) \tag{13}$$

where $\Phi_R(t)$, the probability of adding one more particle, is equal to the fraction of the line available for particle deposition. Since, for a given gap of length $l > 1$, the available length for inserting a new particle is equal to $(l-1)$, the function $\Phi_R(t)$ is equal to

$$\Phi_R(t) = \int_1^\infty (l-1)G_R^0(l,t)\,\mathrm{d}l. \tag{14}$$

Inserting equation (6) in (14) and using equation (13) leads to the following expression for the density:

$$\rho_R(t) = \int_0^t H(u)\,\mathrm{d}u = \frac{\mathrm{e}^{-(2\gamma-R)}}{(R+1)} \int_0^t \mathrm{e}^{-[E_1((R+1)u)+E_1(u)+R\,\mathrm{e}^{-u}]} \frac{\mathrm{d}u}{u^2} \tag{15}$$

which is equivalent to equation (12). The jamming density, $\rho_R(\infty)$, can be calculated by taking the limit for $t \to \infty$ in the latter equation, which thus gives

$$\rho_R(\infty) = \frac{\mathrm{e}^{-(2\gamma - R)}}{(R+1)} \int_0^\infty \mathrm{e}^{-[E_1((R+1)u) + E_1(u) + R\,\mathrm{e}^{-u}]} \frac{\mathrm{d}u}{u^2}. \tag{16}$$

Now, we can easily evaluate the short-time behaviour which is given by $\rho_R(t) = t + \mathrm{O}(t^2)$, while close to the jamming limit $\rho_R(t)$ approaches its saturation value following an algebraic law, which gives

$$\rho_R(\infty) - \rho_R(t) \approx \frac{\mathrm{e}^{-(2\gamma - R)}}{(R+1)} t^{-1}. \tag{17}$$

The asymptotic behaviour of $\rho_R(t)$ is thus similar to that of a conventional RSA. Note also that, for $R = 0$, the function $H(t)$ in equation (9) as well as the density given by equation (15) correspond to the well known car parking problem, where the jamming limit (16) is $\rho_{R=0}(\infty) = 0.747\,59$ [1]. Note that the previous analysis is only valid for finite values of R.

2.2. Monte Carlo simulation

Here we consider briefly the simulation scheme for the deposition process. The procedure is almost described in the definition of the model given above. We consider an off-lattice model where the area covered by the monomer is taken to be equal to 1. The monomers arrive randomly at the line of size L with periodic boundary conditions. Typical lattice sizes used in our simulations are in the range $L = 10^3$–10^5 depending on the value of the parameter R, which is in the range $R = 0$ to 5×10^3. In our simulation experiments no finite-size effect has been observed in the quantities of interest. The corresponding deposition algorithm is as follows. (i) A real number between $0 < \eta < L$ is selected at random, the corresponding segment $\eta, \eta + 1$ is considered. If the deposition place defined by the segment is total or partially occupied the trial ends, i.e. the monomer deposition cannot take place because the deposition area is blocked by an adsorbed adparticle. (ii) The Monte Carlo (MC) time t is increased to $t + \Delta t$. (iii) After monomer deposition we decide at random, with equal probability, the flying direction. (iv) If during the flight the monomer hits another adparticle or ensemble which is already at rest, the flying monomer is frozen in at the collision point.

The MC time increment Δt is defined as $1/L$ in such way that the MC unit time ($t = 1$), on average, involves $L/1$ trials. During the deposition process the following quantities are measured: the density $\rho_R(t)$ as a function of time t and the probability $\Phi_R(t)$, calculated as the ratio between the number of successful deposition attempts and the total number of attempts,

$$\Phi_R(t) = \frac{\Delta n}{L \Delta t} \tag{18}$$

where Δn is the number of particles adsorbed in the interval of time Δt. The jamming density $\rho_R(\infty)$ is calculated as the limit of the density $\rho_R(t)$ for $t \to \infty$ that corresponds to a very large simulation, and to avoid this problem we use a procedure to accelerate the calculation of the jamming state, so with this value of the jamming density we calculate the kinetics of the process. The results were averaged over a number of 10^3 samples, depending on the size of the lattice. The simulations were carried out on the PARIX parallel computer system with eight nodes.

3. Analysis of the results

3.1. The kinetics of hot deposition in the continuum

Figure 3 shows plots of $\rho_R(t)$ against time obtained for different values of R ($0 \leqslant R \leqslant 1000$). The results are obtained for any values of R by Monte Carlo simulations. For small R, the results should be compared with the corresponding numerical solutions of the rate equations. As in the discrete case [18], for early times and low coverage ($\rho_R < 0.4$) there is no appreciable difference in the deposition kinetics when R is varied. Nevertheless, for $\rho > 0.4$ a distinct behaviour is observed for different choices of the parameter R: for a fixed time, the greater is R the higher is ρ. A qualitative understanding of this behaviour can be explained as follows: as the parameter R increases a given adsorbed particle can hit, during the flight, another adparticle or clusters of adsorbed particles with higher probability than in the case of small R; therefore, the number of empty gaps with length $l < 1$ diminishes and the coverage increases. To reinforce this explanation, figure 4 shows plots of $\Phi_R(\rho)$ against density ρ for different values of R. From the figure it is evident that the probability that an incoming particle hits a free area on the line increases with the parameter R, at fixed coverage ρ; the lower curve corresponds to $R = 0$ which is the classical car parking problem. In the opposite limit, for very large values of the parameter R ($R \to \infty$), the probability $\Phi_R(\rho)$ approaches the limiting case $\Phi_R(\rho) = (1 - \rho)$. Inserting this expression for $\Phi_R(\rho)$ in equation (13) and solving, we obtain

$$\rho_\infty(t) = 1 - [1 - \rho_\infty(t)|_{t=0}]\,\mathrm{e}^{-t} \tag{19}$$

where $\rho_\infty(t)|_{t=0}$ is the initial density of particles. Formally, the initial density can be taken to be zero; however, in the limit $R = \infty$ it is necessary to have at least one previous adsorbed particle in order that the deposition process takes place, so $\rho_\infty(t)|_{t=0} \neq 0$ [21]. The asymptotic regime, for very large values of R, is clearly exponential with a full coverage as the jamming state $\rho_\infty(\infty) = 1$. On the other hand, for $R = 0$, the asymptotic regime is power-law dependent with $(\rho_0(\infty) - \rho_0(t)) \propto t^{-1}$ as was previously demonstrated in equation (17). Consequently there should be a crossover between both kinetic regimes. In order to confirm the last assumption, let us define the following function,

$$\Gamma_R(t) = \frac{\rho_R(\infty) - \rho_R(t)}{\rho_R(\infty)}. \tag{20}$$

Figure 5 shows plots of $\Gamma_R(t)$ against time. It appears that a clear straightline behaviour on a semilogarithmic plot figure 5(a) is obtained for large values of R and for times smaller than the crossover time $t < \tau_R$. In the limit $R = \infty$, the crossover time also takes the value $\tau_R = \infty$ and the kinetics become exponential. In figure 5(b), $\Gamma_R(t)$ estimates are plotted on a double logarithmic scale, and it is clear that the data for values of $R < 10$ present a power-law dependence, while for large values of R the early time regime breaks off such a dependence at time $t \approx \tau_R$, recovering the asymptotic power-law dependence at $t > \tau_R$. To calculate the crossover time τ_R, each curve in figure 5(b) is fitted in the power-law region, and from the intersection of the fitting line with the curve corresponding to $R = \infty$ one can obtain τ_R. Figure 6 shows the semilogarithmic plot of the crossover time τ_R against R for large values of R. The data can be reasonably fitted by $\tau_R = a + b \log_{10} R$ with $a = 0.579 \pm 0.001$ and $b = 2.361 \pm 0.002$. A qualitative explanation of this interesting crossover between both asymptotic regimes is also based on the fact that the number of empty gaps with length $l < 1$ disminishes and the coverage increases as the parameter R increases. In this way, the incoming particles are adsorbed without empty gaps between them, so each place on the line is covered by the particles as in the discrete adsorption

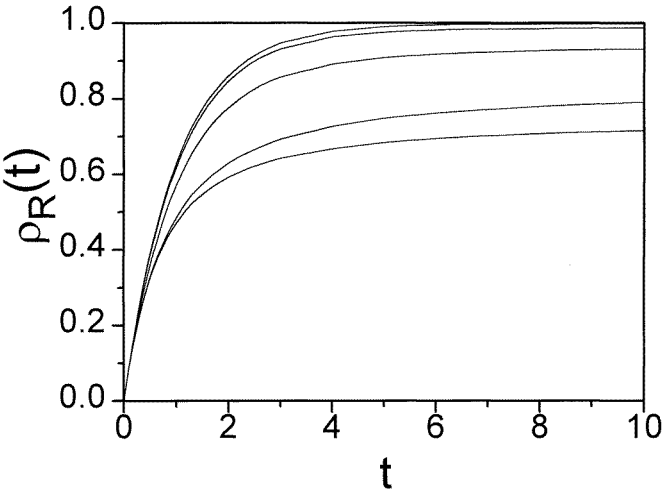

Figure 3. The time dependence of the density $\rho_R(t)$ and different values of the parameter R. Starting from the topmost data, $R = 1000, 100, 10, 1, 0$. Numerical solutions and Monte Carlo simulations coincide for small values of R ($R = 0, 1$).

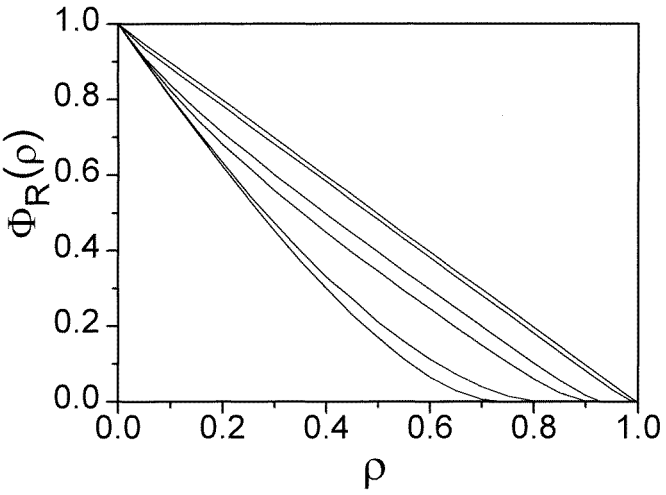

Figure 4. The probability $\Phi_R(\rho)$ against ρ plotted for different values of R. Starting from the topmost data, $R = 1000, 100, 10, 5, 1, 0$.

process. It is interesting to emphasize that, in our study, the crossover from power-law to exponential kinetics is a novel situation which is inherent to the 'hot' deposition mechanism in the continuum.

3.2. The jamming state

One interesting aspect of 'hot' transient mobility is the R-dependence of the jamming density in the continuum, as well as in the discrete deposition process. In the discrete process, the dependence of the jamming coverage with R, for hot dimer adsorption, is given by a power law $|\theta_\infty(\infty) - \theta_R(\infty)| \propto R^{-x}$, where the exponent is $x \approx 0.9$ with $\theta_\infty(\infty) = 1$ in one

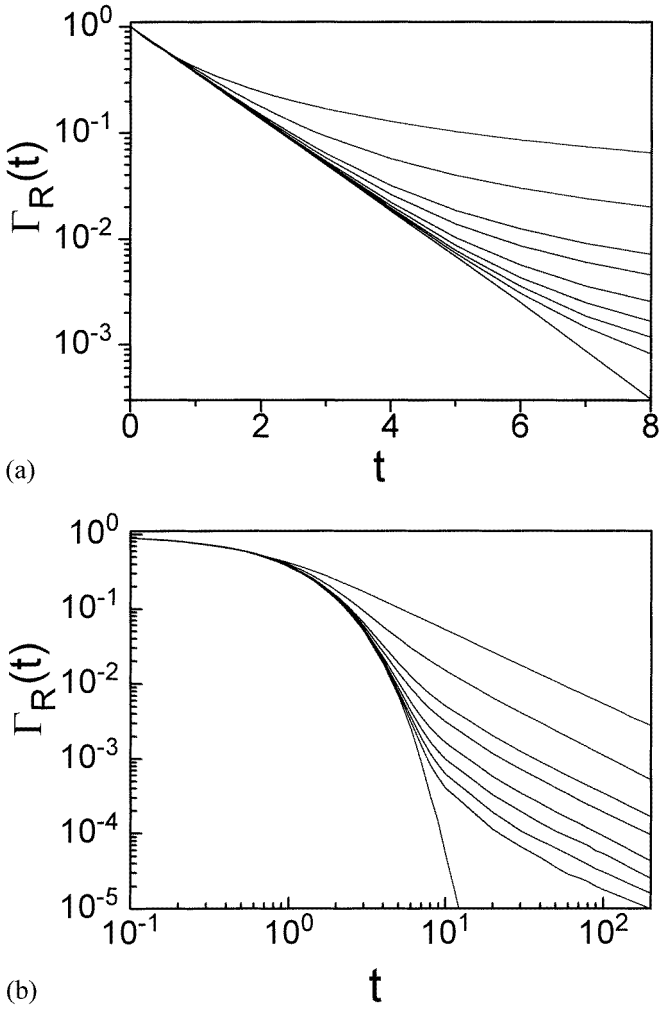

Figure 5. (a) A semilogarithmic plot of the time dependence of $\Gamma_R(t)$ for different values of the parameter R. Starting from the top-most data, $R = 1$, 10, 50, 100, 250, 500, 1000, 2000 and 5000. (b) As in (a) but plotted on a double logarithmic scale. The crossover times are calculated from figure 4 by fitting the power-law region and intersecting the curve corresponding to $R = 5000$ ($R \approx \infty$).

dimension and $x \approx 0.5$ with $\theta_\infty(\infty) = 0.943$ in a two-dimensional square lattice [18, 19]. In contrast with the simple power-law dependence, the jamming density for hot dimer deposition in the continuum goes as $\rho_R(\infty) \propto R/(R+1)$ for large values of R, presenting finite discontinuities of $\rho_R(\infty)$ near the integer values of the flight distance R [24].

To analyse the R-dependence of 'hot' monomer deposition, we show in figure 7 a plot of $\rho_R(\infty)$ against $R/(R+1)$. One can observe that the jamming density approaches to $\rho_R(\infty) \propto \frac{1}{2}R/(R+1)$ for large values of R. The limit values of the jamming density, as a function of R, are according to the previous analysis. In fact for $R = 0$, we have the classical car parking model, where the jamming density is $\rho_0(\infty) = 0.747\,59$ [9] and for $R \to \infty$ the jamming density tends to 1 [20, 21]. Note that the analytical results are

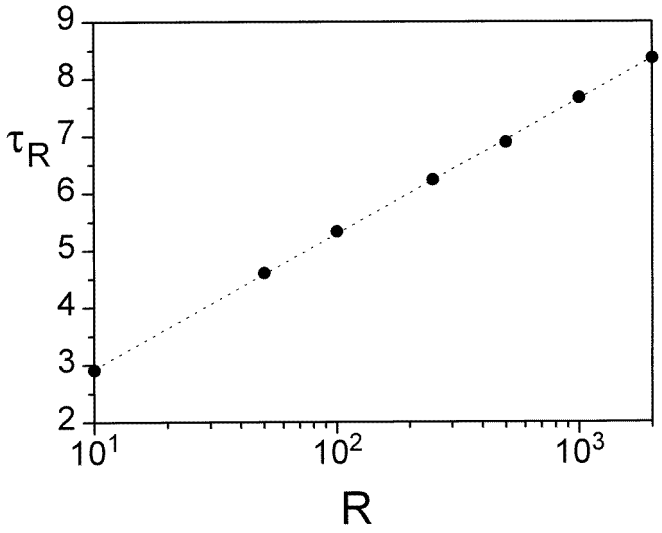

Figure 6. The crossover time τ_R as a function of R.

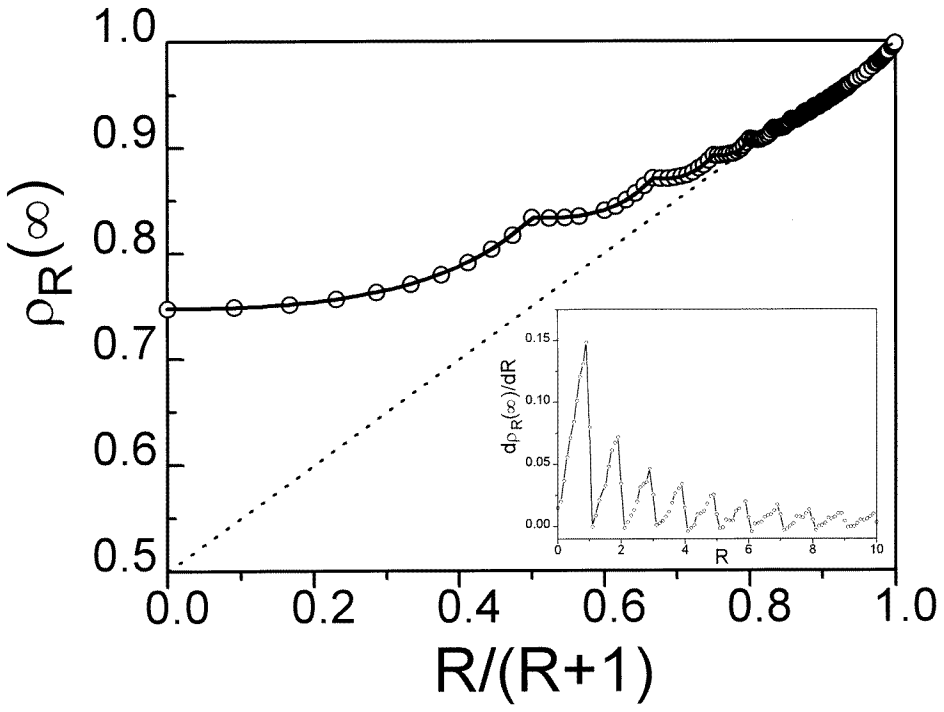

Figure 7. The jamming density $\rho_R(\infty)$ plotted against $R/(R+1)$. Numerical solutions (dashed line) are compared with Monte Carlo simulations (symbols) for small values of R. In the inset we show the derivative of the jamming density $\mathrm{d}\rho_R(\infty)/\mathrm{d}R$ plotted against R. We can observe the finite discontinuities for integer values of R.

in perfect agreement with the simulations; however, for $R > 4$ the time required for the numerical solution of the rate equations is larger than that for the simulation.

One of the main features of the curve in figure 7 is the behaviour of the first derivative of the jamming density $\mathrm{d}\rho_R(\infty)/\mathrm{d}R$ as a function of the parameter R, which presents finite discontinuities in the neighbourhood of integer values of R (see the inset in figure 7), and which are due to the discontinuities of the GDF at $l = R - \mathrm{int}(R)$. To probe this, let us consider the following argument: the gap distribution function is $G_R(l, \infty) \neq 0$ only for those values of $l \in (0, 1)$; therefore, the expression for the jamming density $\rho_R(\infty)$ can be written as

$$\rho_R(\infty) = 1 - \int_0^1 l G_R(l, \infty)\, \mathrm{d}l. \tag{21}$$

Figure 8 shows a plot of $G_R(l, \infty)$ as a function of l for two different values of the parameter R; the gap distribution functions coincide in all ranges of l except for those values between $R \leqslant l \leqslant R'$. Then it follows from figure 8 that the difference $G_{R'} - G_R \approx 0$ except for $R \leqslant l \leqslant R'$; therefore, by using equation (14) we get

$$\rho_R(\infty) - \rho_{R'}(\infty) = -\int_R^{R'} l[G_{R'}(l, \infty) - G_R(l, \infty)]\, \mathrm{d}l. \tag{22}$$

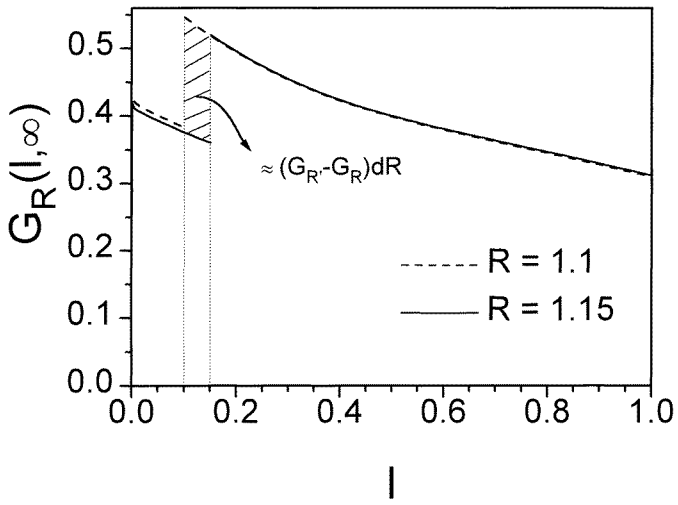

Figure 8. A plot of $G_R(l, \infty)$ against l for two different values of the parameter R.

If we take $R' = R + \mathrm{d}R$ the last expression can be approximated by

$$\rho_R(\infty) - \rho_{R'}(\infty) \approx R(G_{R+\mathrm{d}R}(l, \infty) - G_R(l, \infty))\, \mathrm{d}R \tag{23}$$

and taking $\mathrm{d}R \to 0$ we obtain

$$\frac{\mathrm{d}\rho_R(\infty)}{\mathrm{d}R} = -f(R)\Delta G_R \tag{24}$$

where $f(R)$ is defined as

$$f(R) = \begin{cases} R & \text{if } R < 1 \\ R - \mathrm{int}(R) & \text{if } R \geqslant 1. \end{cases} \tag{25}$$

The value of the derivative, equation (24), will be different, approaching a given integer value of R from the right or left according to equation (25). Hence the origin of the discontinuities is proved.

4. Conclusions

In this paper, we have presented a model for the deposition of hot monomers in the continuum. By means of Monte Carlo simulations and analytical approaches we have studied so-called 'hot' monomer adsorption in the continuum for finite flight distances R. We have developed the kinetic rate equations for the gap distribution functions and calculated the density as a function of time. The numerical solutions of the rate equations are in good agreement with the Monte Carlo simulation results; however, for $R > 4$ we observe that the computational time for the numerical integration of the rate equation is larger than the time required for the Monte Carlo simulation.

As novel feature, a crossover between the power-law asymptotic approach as a function of time $(\rho_R(\infty) - \rho_R(t)) \propto t^{-1}$ for the density at small R and the exponential behaviour of the asymptotic regime of the density for very large R is obtained. This effect which is inherent to the 'hot' transient mobility can be explained by the fact that the number of empty gaps with length $l < 1$ diminishes and the coverage increases as the parameter R increases. The jamming density is a piecewise continuous function of R, but $\mathrm{d}\rho_R(\infty)/\mathrm{d}R$ has finite discontinuities at integer values of R. On the other hand, for large values of R the jamming density is given by a simple law, $\rho_R(\infty) \propto \frac{1}{2}R/(R+1)$.

Acknowledgments

This work is partially supported by the CONICET (Argentina) and Fundacion Antorchas (Argentina). The European Economic Community, Project ITDC-240, is greatly acknowledged for the provision of valuable equipment.

Appendix

A.1 Rate equations for $R > 1$

In the case of $R > 1$, examination of the time evolution of the gaps also leads to a set of closed equations for the GDF; however, the number of rate equations grows linearly with R, so therefore there is a critical value of R where the computational time required to solve the rate equations increases to more than the time corresponding to the Monte Carlo simulation; in our numerical experience such a critical value is $R \approx 4$. Nevertheless, it is interesting to present here the derivation of the rate equations which govern the kinetics of the process. Thus, for a given interval of length $l > R$, the gap distribution function evolves according to:

for $R < l$,

$$\frac{\partial G_R^0(l,t)}{\partial t} = -(l-1)G_R^0(l,t) + RG_R^0(l+1,t) + \int_{l+1}^{l+R+1} G_R^0(l',t)\,\mathrm{d}l' + 2\int_{l+R+1}^{\infty} G_R^0(l',t)\,\mathrm{d}l'. \tag{A.1}$$

In the latter equation the terms on the right-hand side are equivalent to those in equation (3). Now, for gaps with length between $(R-i) < l < (R-(i-1))$, with $i = 1, 2, 3, \ldots, (m-1)$ (with $m = \mathrm{int}(R)$), the corresponding rate equation is given by

$$\frac{\partial G_R^i(l,t)}{\partial t} = -(l-1)G_R^i(l,t) + lG_R^{(i-1)}(l+1,t) + \int_{l+R+1}^{\infty} G_R^0(l',t)\,\mathrm{d}l' \tag{A.2}$$

where the first term on the right-hand side is due to the destruction of the gap with length l by deposition of a particle in the $l-1$ possible place. The second term describes the

creation of such gaps from those with length $l' = l+1$ by deposition of one monomer in the l possible inner places. The last term is the contribution of the gaps with length $l' \geqslant l+R+1$. Next, we consider the evolution of the gaps with length between $1 < l < (R-m+1)$, which is described by

$$\frac{\partial G_R^m(l,t)}{\partial t} = -(l-1)G_R^m(l,t) + lG_R^{(m-1)}(l+1,t) + \int_{l+R+1}^{\infty} G_R^0(l',t)\,\mathrm{d}l' \tag{A.3}$$

where the description of the terms on the right-hand side are equivalent to those in equation (A.2). Now, we consider the evolution of these gaps which cannot be destroyed in the process; the length of such gaps are always $l < 1$. One has to distinguish two case: for $(R-m) < l < 1$ we have

$$\frac{\partial G_R^{m+1}(l,t)}{\partial t} = lG_R^{m-1}(l+1,t) + \int_{l+R+1}^{\infty} G_R^0(l',t)\,\mathrm{d}l' \tag{A.4}$$

and finally, for $0 < l < (R-m)$, the rate equation is

$$\frac{\partial G_R^{m+2}(l,t)}{\partial t} = lG_R^{m}(l+1,t) + \int_{l+R+1}^{\infty} G_R^0(l',t)\,\mathrm{d}l'. \tag{A.5}$$

The rate equations may be solved by inserting the ansatz of equation (6) into (A.1). The function $H(t)$ obtained by this procedure is the same as given in equation (9). Now, let us define the following function,

$$\chi(R,l,t) = \int_{l+R+1}^{\infty} G_R^0(l',t)\,\mathrm{d}l' = tH(t)\,\mathrm{e}^{-(l+R)t}. \tag{A.6}$$

By using the function χ, the set of equations (A.2) and (A.3) can be rewritten iteratively as

$$\frac{\partial G_R^n(l,t)}{\partial t} + (l-1)G_R^n(l,t) = lG_R^{n-1}(l+1,t) + \chi(R,l,t) \tag{A.7}$$

where $n = 1,\ldots,m$, the solution of which gives

$$G_R^n(l,t) = \mathrm{e}^{-(l-1)t}\int_0^t \mathrm{e}^{(l-1)t}[lG_R^{n-1}(l+1,t) + \chi(R,l,t)]\,\mathrm{d}t. \tag{A.8}$$

The density $\rho_R(t)$ can be evaluated inserting the expression for $G_R^j(l,t)$, with $j = 0,\ldots,m+2$, in equation (2) resulting in

$$\begin{aligned}\rho_R(t) = 1 &- \int_0^{(R-m)} lG_R^{m+2}(l,t)\,\mathrm{d}l - \int_{(R-m)}^{1} lG_R^{m+1}(l,t)\,\mathrm{d}l \\ &- \int_1^{(R-(m-1))} lG_R^{m}(l,t)\,\mathrm{d}l - \cdots - \int_R^{\infty} lG_R^0(l,t)\,\mathrm{d}l.\end{aligned} \tag{A.9}$$

Finally, the jamming density can be obtained by taking the limit $t \to \infty$ in the last equation, which gives

$$\rho_R(\infty) = 1 - \int_0^{R-m} lG_R^{m+2}(l',\infty)\,\mathrm{d}l' - \int_{R-m}^{1} lG_R^{m+1}(l',\infty)\,\mathrm{d}l'. \tag{A.10}$$

References

[1] Evans J W 1993 *Rev. Mod. Phys.* **65** 1281
[2] Bartelt M C and Privman V 1991 *Int. Mod. Phys.* B **5** 2883
[3] Gonzalez J J, Hemmer P C and Hoye J S 1974 *Chem. Phys.* **3** 228
[4] Privman V, Wang J-S and Nielaba P 1991 *Phys. Rev.* B **43** 3366
[5] Evans J W and Nord R S 1985 *J. Stat. Phys.* **38** 681
[6] Talbot J, Tarjus G and Schaaf P 1989 *Phys. Rev.* A **40** 4808
[7] Schaaf P and Talbot J 1989 *Phys. Rev. Lett.* **62** 175
[8] Viot P, Tarjus G and Talbot J 1993 *Phys. Rev.* E **48** 480
[9] Renyi A 1963 *Sel. Trans. Math. Stat. Prob.* **4** 205
[10] Onoda G Y and Linigier E G 1986 *Phys. Rev.* A **33** 715
[11] Privman V and Nielaba P 1992 *Europhys. Lett.* **18** 673
[12] Nielaba P, Privman V and Wang J-S 1991 *J. Phys. A: Math. Gen.* **23** L1187
Nielaba P and Privman V 1992 *Mod. Phys. Lett.* B **6** 533
[13] Nielaba P, Privman V and Wang J-S 1994 *Ber. Bunsenges. Phys. Chem.* **98** 451
[14] Nazzarro M S, Ramirez Pastor A J, Riccardo J L and Pereyra V 1997 *J. Phys. A: Math. Gen.* **30** 1925
[15] Mann E K, Wojtaszczyk P, Senger B, Voegel J-C and Schaaf P 1995 *Europhys. Lett.* **30** 261
[16] Brune H, Wintterlin J, Behm R J and Ertl G 1992 *Phys. Rev. Lett.* **68** 624
Brune H, Wintterlin J, Trost J, Ertl G, Wiechers J and Behm R J 1993 *J. Chem. Phys.* **99** 2128
[17] Weiss P S and Eigler D M 1992 *Phys. Rev. Lett.* **69** 2240
[18] Pereyra V D and Albano E 1993 *J. Phys. A: Math. Gen.* **26** 4175
[19] Albano E and Pereyra V D 1993 *J. Chem. Phys.* **98** 10 044
[20] Pereyra V D, Albano E and Duering E 1993 *Phys. Rev.* E **48** R3229
[21] Privman V 1993 *Europhys. Lett.* **23** 341
[22] Pereyra V D and Albano E 1993 *Appl. Phys.* A **57** 291
[23] Albano E and Pereyra V D 1994 *J. Phys. A: Math. Gen.* **27** 7763
[24] Linares D and Pereyra V 1996 *Phys. Rev.* E **54** 617
[25] Pagonabarraga I, Bafaluy J and Rubi J M 1997 *Phys. Rev. Lett.* **75** 461
[26] Swendsen R H 1981 *Phys. Rev.* A **24** 504
[27] Hinrchsen E L, Feder J and Jossang T 1986 *J. Stat. Phys.* **44** 793
[28] Talbot J and Ricci S M 1992 *Phys. Rev. Lett.* **68** 958